Optical study of CdS- and ZnS-passivated CdSe nanocrystals in gelatin films

2007 J. Phys.: Condens. Matter 19 386237

(http://iopscience.iop.org/0953-8984/19/38/386237)

IOP PUBLISHING JOURNAL OF PHYSICS: CONDENSED MATTER

J. Phys.: Condens. Matter **19** (2007) 386237 (9pp) doi:10.1088/0953-8984/19/38/386237

Optical study of CdS- and ZnS-passivated CdSe nanocrystals in gelatin films

A E Raevskaya[1], A L Stroyuk[1], S Ya Kuchmiy[1], V M Dzhagan[2], M Ya Valakh[2] and D R T Zahn[3]

[1] Institute of Physical Chemistry, National Academy of Sciences of Ukraine, prospekt Nauky 31, Kyiv 03028, Ukraine
[2] Institute of Semiconductors Physics of National Academy of Sciences of Ukraine, prospekt Nauky 41, Kyiv 03028, Ukraine
[3] Institut für Physik, Technische Universität, D-09107 Chemnitz, Germany

E-mail: dzhagan@isp.kiev.ua

Received 12 February 2007, in final form 24 May 2007
Published 6 September 2007
Online at stacks.iop.org/JPhysCM/19/386237

Abstract

CdSe nanocrystals were synthesized in aqueous solutions using gelatin as a stabilizer. An appreciable improvement of photoluminescence efficiency of nanocrystal-containing polymeric films was achieved by passivation of as-formed nanocrystals in solutions with CdS and ZnS. The passivation-induced variation of the photoluminescence efficiency and its maximum position was found to be dependent on the total volume of the passivating material and the sequence of the reagents involved. The photoluminescence of both unpassivated and passivated nanocrystals was noticeably (∼200 meV) red-shifted from the first absorption maxima. A possible origin of the emission observed is discussed.

1. Introduction

Semiconductor nanocrystalline materials have been intensively studied within the past two decades, and unique physical properties due to quantum confinement effects have been reported [1]. In nano-sized systems with the portion of the surface atoms of up to 70–90% compared to that of the corresponding bulk, surface states play a crucial role in determining their physical properties. The surface of nanocrystals (NCs) is constituted by atoms that are not fully coordinated and, hence, are highly active. These surface atoms act like defect states unless they are passivated by either organic ligands or wider-bandgap semiconductor materials [1, 2]. In the latter case so-called 'core–shell' NCs are obtained [1]. Organic ligands cannot passivate both cationic and anionic surface sites of the core [3]. Nanoparticles passivated by inorganic shell structures are more robust than organic-passivated nanocrystals and, therefore, have greater tolerance with respect to the processing conditions necessary for incorporation into solid structures [4].

For efficient surface passivation, core nanoparticles are capped with a wider-bandgap material, with the conduction band energy of the shell being usually higher than that of the core material and with the valence band energy of a capping material being lower (type-I heterostructure [1]). Due to the presence of the wider-bandgap capping material, the photogenerated excitons remain localized and are forced to recombine while spatially confined in the core. As non-radiative decay channels through surface states are not accessible for charge carriers in the core–shell structures, these structures show higher photoluminescence (PL) quantum yield [2, 3, 5–10], lower fluorescence lifetime [9], and many other benefits related to the tuning of the bandgap in two materials.

In the present paper we discuss the synthesis of aqueous CdSe sols with tuneable NC size and size distribution from sodium selenosulfate and subsequent passivation of the surface of CdSe NCs with cadmium or zinc sulfide. Absorption and PL spectral measurements were performed at room temperature for the characterization of the obtained core–shell nanostructures.

2. Experimental details

Reagent grade $CdSO_4$, $Zn(NO_3)_2$, Na_2SO_3, Na_2S, Se and gelatin were purchased from Aldrich and used without further purification. Aqueous sodium selenosulfate solutions (0.2 M) were prepared via dissolution of powdered selenium in hot (80–90 °C) aqueous Na_2SO_3 solution, while maintaining the molar ratio [Se]:[Na_2SO_3] = 1:3.

2.1. CdSe nanocrystal synthesis

A solution containing cadmium sulfate (0.06 M) and gelatin (5 mass%) was added dropwise at room temperature to the solution of 0.06 M sodium selenosulfate and 5 mass% of gelatin. The resulting mixture was then placed into a refrigerator at 4 °C for gelation and left for ageing and CdSe nanocrystal formation. Diffusion restriction in the gelatin gels favours the formation of small NCs with narrow size distribution. Nanocrystal growth stopped usually after 20–24 h of gel ageing. Aged gels were then cut into small pieces and immersed in distilled water at 4–10 °C for 14–18 days, so that all water-soluble salt residues were removed from the gels. After the dialysis and filtration the gels were dissolved in a measured water volume at 30 °C to give 0.01 M colloidal CdSe solution stabilized by 5 mass% of gelatin. Detailed characterization of the gelatin-capped CdSe nanocrystals, synthesized from Na_2SeSO_3, can be found in [11, 12].

2.2. Surface passivation of CdSe NCs with CdS or ZnS

Measured volumes of 0.01 M $CdSO_4$ or $Zn(NO_3)_2$ solutions were added to the gelatin-stabilized CdSe colloids. The colloids were kept with intense stirring for 5–10 min and then an amount of the sodium sulfide 0.1 M solution equimolar to the metal ion was added dropwise while stirring the colloidal solution. A number of samples was prepared where sodium sulfide was added prior to the metal salt addition (table 1).

2.3. Preparation of the films with CdSe NCs

Glass-anchored films were prepared from each reference colloidal solution in the following way: 2.5 ml of a colloidal solution were deposited onto a previously cleaned 2.0 cm^2 glass plate and left for drying at 18–20 °C for several days.

Table 1. Summary of the absorption and PL data for the studied samples.

Sample	Absorption maximum, $eV \pm 0.002$ eV (nm $\pm$ 1 nm)	PL maximum, eV $\pm$ 0.002 eV (nm $\pm$ 1 nm)	PL FWHM, meV $\pm$ 2 meV	PL intensity, au ($\pm$0.2)
CdSe non-passivated	2.490 (498)	2.250 (551)	195	1
[CdSe]:[CdS] = 1:0.5 Cd then S	2.470 (502)	2.238 (554)	192	1.4
[CdSe]:[CdS] = 1:1 Cd then S	2.455 (505)	2.230 (556)	190	1.8
[CdSe]:[CdS] = 1:1 S then Cd	2.460 (504)	2.234 (555)	170	2.8
[CdSe]:[CdS] = 1:3 S then Cd	2.410 (515)	2.183 (568)	175	1.7
[CdSe]:[ZnS] = 1:10 Zn then S	2.408 (515)	2.179 (569)	140	4.2
[CdSe]:[ZnS] = 1:10 S then Zn	2.398 (517)	2.157[a] (575)	200[a]	0.3

[a] The error is different from that indicated in the header of the table and is equal to 0.005 eV.

2.4. Optical measurements

Absorption spectra of the films were recorded using a Specord M40 double-beam spectrophotometer. Photoluminescence (PL) spectra were recorded at room temperature using a Dilor XY 800 triple monochromator equipped with a charge-coupled device camera for multichannel detection. The PL spectra were excited with a 441.7 nm line of a He–Cd laser.

3. Results and discussion

Absorption and PL maxima of the initial CdSe NCs (figure 1) are significantly shifted to higher energies, as compared to the absorption edge of bulk CdSe (712 nm, $E_g = 1.74$ eV), indicating the formation of CdSe NCs with pronounced quantum size effect [13]. From the position of the first absorption maximum at 2.49 eV the average diameter d of the non-passivated NCs was estimated to be 2.6 ± 0.3 nm, using the dependence of $E_g(d)$ reported in the literature [14–16].

The PL spectrum of the initial CdSe NCs consists of a relatively sharp near-bandgap emission peak centred at about 2.26 eV and of a weak broad (FWHM about 400 meV) band centred around 1.8 eV, significantly red-shifted from the NC absorption edge and evidently caused by surface-state-mediated recombination [2, 17]. Following the procedure developed in [18], the CdSe NC size dispersion was estimated from the absorption and PL spectra to be about 15%. This value is much higher than in the best samples of TOPO-assisted synthesis [3, 5, 19], but quite good as compared to similar samples in polymers or in inorganic glasses [20, 21]. It should be mentioned that no post-synthesis size selection was made for the present samples.

As seen from figure 1, the absorption and emission spectra shift to lower energies upon passivation with CdS. This shift has been observed for different core–shell materials and is explained by a partial tunnelling of the electron wavefunction of the core into the shell [3, 22]. The magnitude of the shift is expected to be larger for the shells of larger thickness [3, 22].

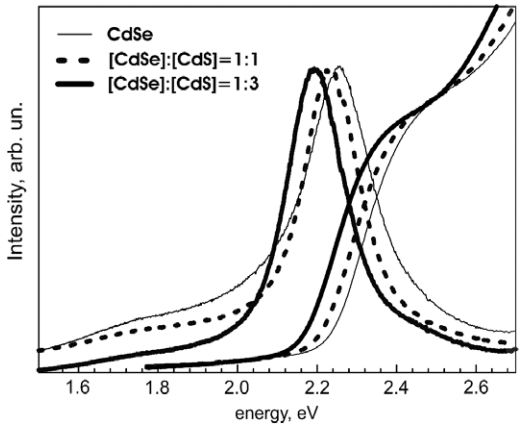

Figure 1. Normalized absorption and PL spectra of CdSe and CdSe/CdS NCs obtained by the 'S then Cd' scheme, with final ratio of [CdSe]:[CdS] = 1:1 (dotted) and 1:3 (thick solid). The initial concentration of CdSe in all cases was 1.0×10^{-3} M.

It is clearly seen in figure 1 for the samples with different thicknesses of the CdS shell, when reagents containing sulfur atoms were added before those containing cadmium ('S then Cd'-scheme). The shifts of both the absorption threshold and emission maximum are proportional to the volume of the passivating material (table 1). The addition of CdS according to the 'Cd then S' scheme with concentration of [CdSe]:[CdS] = 1:0.5 and [CdSe]:[CdS] = 1:1 causes very close shifts in the absorption and emission spectra (table 1), evidently because of small differences in the volume of passivating material added in these two samples. The addition of equal volumes (1.0×10^{-3} M) of CdS results in nearly the same shift for both 'S then Cd' and 'Cd then S' schemes (table 1).

The effect of ZnS passivation on the optical spectra of CdSe NCs is illustrated in figure 2. The same volume of ZnS ([CdSe]:[ZnS] = 1:10) added to the solution in the above two schemes results, similarly to the CdS shell, in almost identical shifts of the absorption and PL maximum, but the difference in the PL intensity is dramatic and will be discussed below.

Figure 2 also illustrates the effect of the bandgap of the shell material on the optical spectra. The shifts in the spectra for the samples with concentration ratios of [CdSe]:[CdS] = 1:3 and [CdSe]:[ZnS] = 1:10 are very close. This is quite understandable in view of the band structure of both kinds of core–shell NCs. As ZnS possesses a bandgap much larger (3.7 eV) than CdS (2.4 eV), a much thicker ZnS shell is required to obtain a comparable spreading of the electron wavefunctions into the shell, and, therefore, a comparable shift in the optical spectra.

Note that the formation of the passivating shells was additionally confirmed by resonant Raman scattering experiments reported elsewhere [24, 41]. The shifts in the absorption and emission spectra of the passivated samples, attributed to changes in the shell thickness, correlate with the frequency and intensity of the Raman peak caused by lattice vibrations within the passivating layer. Additionally, based on a higher Raman frequency, the higher PL intensity for the 'Zn then S' sample, compared to the 'S then Zn' one, can be explained by a less intermixed and more strained shell in the former case [41].

Although very close shifts in PL and absorption spectra were found for two passivation schemes applied within the present synthesis, this is not generally the case when comparing different preparation techniques. A large scatter of the shifts can be found in the literature for both CdSe/CdS and CdSe/ZnS NCs (figure 3). These observations indicate the effect of a

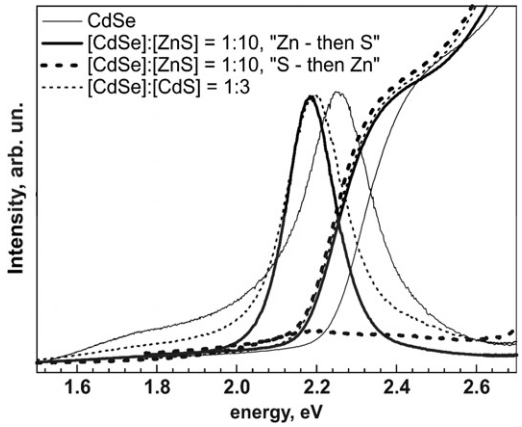

Figure 2. Normalized absorption and PL spectra of CdSe and CdSe/ZnS NCs passivated according to 'Zn then S' and 'S then Zn' schemes with final ratio of [CdSe]:[ZnS] = 1:10 in both cases. The corresponding spectra for CdSe/CdS with [CdSe]:[CdS] = 1:3 are shown for comparison (the PL spectrum for 'S then Zn' was not scaled because of insufficient intensity in the as-measured spectrum).

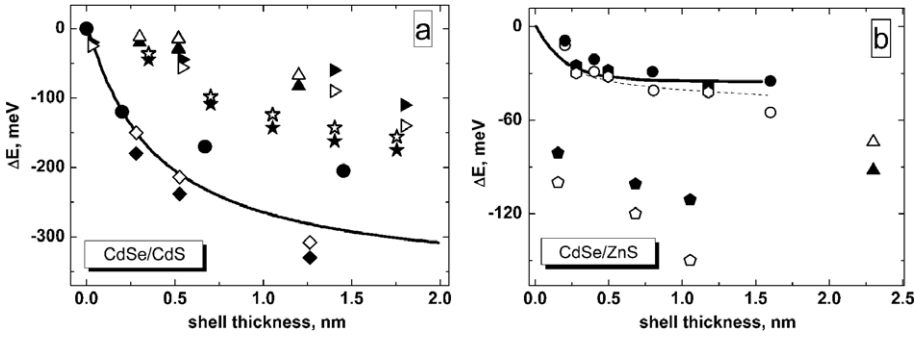

Figure 3. CdS- (a) and ZnS- (b) passivation-induced shift of absorption and PL maxima for CdSe NCs observed in present experiment and by other authors. Filled symbols denote absorption and open denote PL shifts, d stands for CdSe core diameter. ●, ○—d = 2 nm [22]; ◀, ◁—d = 2.3 nm [1]; ▶, ▷—d = 3 nm [1]; ◆, ◇—d = 2.1 nm [33]; ⟡, ⟐, ◈—d = 1.8, 2.1, 2.8 nm [33]; ★, ☆—d = 3.5 nm [34]; ▼, ▽—d = 3.8 nm [35]; ⬟, ⬠—d = 4 nm [23]; ⬢, ⬡—d = 3.8 nm [35]; ▲, △—present work, d = 2.6 nm. Dependencies calculated in [22] for absorption (solid lines) and PL (dashed line) and d = 2 nm are shown as well.

synthetic route and medium applied on the value of resultant red-shift PL or absorption. Note that a comparison of different passivation procedures is reasonable only for NCs with the same (or very close) diameter d of the core and shell thickness. Among possible reasons for large deviations observed may be the following: initial charge and strain state of the bare CdSe NC surface; structure of the shell formed (defects, strain); core–shell alloying. The experimental proofs of the alloying, in particular, and its effect on the PL intensity and FWHM in present CdSe/ZnS NCs were obtained from a Raman spectroscopy study [41].

The effect of the shell formation on the PL spectra is revealed, along with the red-shift, in a remarkable increase in the intensity of the near-bandgap emission—by a factor of 1.4 up to 4.2. This effect is sensitive to the volume of the passivating material. Thus, for the 'Cd then S' scheme the intensity increases proportionally to the shell thickness (table 1). Simultaneously,

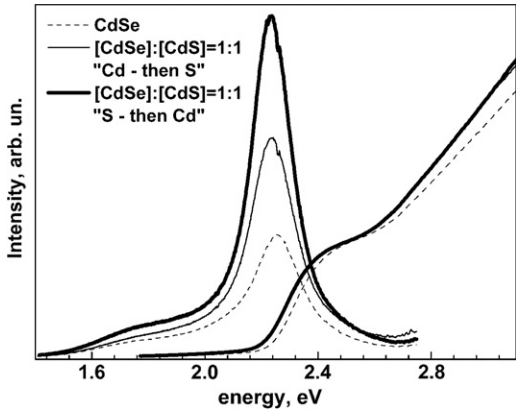

Figure 4. Absorption and PL spectra of CdSe and CdSe/CdS NCs passivated according to 'Cd then S' and 'S then Cd' schemes with a final ratio of [CdSe]:[CdS] = 1:1 in both cases.

increasing the shell volume from 1:1 to 1:3 in the 'S then Cd' scheme, a drop in intensity is observed by a factor of 1.6.

Another important factor is which sort of atoms is added first—metal or sulfur. For the same volume of the shell-forming reagents (1:1) in the case 'Cd then S' much higher PL intensity is achieved than in the case when the scheme 'S then Cd' is applied (figure 4), while the shift of the absorption and emission maxima is very close in both cases (table 1).

From these results and a number of other studies [3, 22, 25], it follows that there exists an optimal, in view of the light emission properties, thickness of the shell, which is different for every particular method of NC preparation and passivation.

The 'right' reagent addition sequence seems to be even more important for the case of the ZnS shell. Thus, the 'Zn then S' addition scheme gives a PL increase by a factor of 4.2 while the opposite sequence quenches the PL by a factor of 3 (see table 1). The latter fact may also be a consequence of the existence of the optimal thickness for every passivation scheme (sequence of reagents), as in the above case of CdS shells. A different sequence of addition of reagents can cause a different number or even nature of defects to be created in the shell, leading to a significant difference in the PL efficiency as for the pair of CdSe/ZnS samples in the present study. Raman spectroscopy study on the present CdSe/ZnS NCs shows that the drop in PL intensity after 'S then Zn' passivation may be a result of a strong intermixing between the core and shell during the shell formation [41].

Along with the increase of the near-bandgap PL, the shell growth leads to a decrease of the relative intensity of the surface-related PL band. The effect is most pronounced for the 'Zn then S' passivation, when this band is completely eliminated (figure 2). The increase of the overall PL intensity from the samples indicates a reduction of the number of non-radiative recombination routes. The quenching of the defect PL with a simultaneous increase of the near-bandgap PL is an evidence of the efficient passivation of the defect states involved in the 'red' emission from the CdSe NCs. No observable change in the position of the remaining surface-related band was detected after the passivation.

The procedure of shell deposition is usually observed to induce some broadening of the PL bands, which is supposed to result from the non-homogenous shell thickness distribution both among the NCs and on the surface of each NC [22, 25]. We observed passivation of the CdSe NCs to result in a narrowing of the excitonic emission bands. The decrease of the PL

band width in this case reaches up to 25% for the CdSe/ZnS sample using the 'Zn then S' shell deposition scheme. A possible reason for the narrowing of excitonic PL bands may be the cubic structure of the NCs prepared by the given synthetic route, which was confirmed in an earlier work by x-ray measurements [11]. In wurtzite-type NCs, studied in [3, 22, 25], the opposite trend was observed for the PL band width, namely an FWHM increase after the shell deposition. The zinc-blende (cubic) structure is more symmetrical compared to wurtzite (hexagonal) and can give more homogenous shell thickness. The observed band narrowing can alternatively arise when not all NCs are uniformly passivated and their contribution to the PL spectrum is weaker. This assumption was partially confirmed by selective sampling of the larger NCs with an excitation wavelength $\lambda_{exc} = 514.5$ nm. Under this (resonant) excitation the PL spectrum exhibits a near-bandgap emission band narrowing by a factor of about two, as compared to the non-resonant excitation using 441.7 nm light. Another difference under resonant excitation of large NCs is that the FWHM of the PL band slightly increases for the capped NCs, similarly to what is commonly reported in the literature [23]. Thus the narrower PL bands of the passivated samples compared to unpassivated at 441.7 nm excitation may be evidence of the size-selective passivation procedure involved. However, the maxima of the emission peaks for both excitation wavelengths are very close for all the samples. Only at $\lambda_{exc} = 530$ nm was a shift of the PL maximum noticed.

Under non-resonant excitation, the value of the Stokes shift ΔS of the near-bandgap PL maximum from the absorption maximum was found to be quite large—about 200 meV for all samples. The ΔS values usually observed are within 100 meV, but very large shifts (up to 300 meV) were also reported [26, 20, 27].

The origin of the Stokes shift in CdSe NCs is mostly explained based on a 'dark exciton' model [19, 28, 29], although the model involving recombination through surface traps was extensively applied, especially to explain large ΔS values [17, 28, 30–32]. The reason for a large ΔS value could, therefore, be found from establishing the nature of the processes responsible for the observed near-band-edge PL.

The fact that the PL intensity can be increased by appropriate passivation with CdS or ZnS can hardly be a proof for either intrinsic (excitonic) or surface-related origin of the PL. When such a passivation (partially) reduces the channel(s) of non-radiative recombination, this can result in an enhancement of any kind of radiative recombination channels—either excitonic or mediated by (shallow) traps.

The preliminary time-resolved PL measurements, which will be reported in detail in the forthcoming paper, revealed an increase of a mean decay time in the NCs after passivation, in agreement with the increase of absolute PL intensity after shell deposition. From fitting the decays with four exponentials, decay components of 0.5–0.6, 2.5–3.0, 10–15 and 40–70 ns were derived. The first two components are obviously related to the matrix emission, which also contributes to the spectrum in the spectral region of the NC-related PL, as they were also derived from the PL decay of gelatin film without NCs. Only the third and fourth components changed noticeably after passivation, and can, therefore, be related to the NC PL. Relatively long decay times at a relatively low PL efficiency may be evidence of the radiative recombination occurring through the shallow traps [36, 37]. This could easily explain a large Stokes shift of the NC emission [36]. However, a quite broad range of both excitonic and trap emission decay times was reported in the literature [36–40]; this time is obviously strongly dependent on the NC size, the kind of stabilizer and surfactant used and other factors.

Moreover, a solid argument given in [19] for the possibility of large Stokes shifts of the excitonic PL does not allow us to exclude such a possibility in our case. Note that according to the model [19] the magnitude of ΔS increases with a decrease of the mean NC size and with an increase of the size dispersion. The dependence $\Delta S(d)$ becomes extremely steep for d below

3 nm and could evidently reach values close to 200 meV for the present NCs with a mean size of 2.6 nm and size dispersion of around 15% (see figure 11 in [19]).

Further time-resolved and low-temperature steady state PL measurements will be performed for better understanding of the physical processes involved in the photoluminescence of the CdSe NCs reported here.

4. Conclusions

CdSe NCs possessing quite narrow near-bandgap emission bands were synthesized in aqueous solution under relatively mild conditions from sodium selenosulfate with gelatin as a stabilizer. In order to further improve the luminescence properties of the NCs, they were passivated with CdS or ZnS. Passivation results in a shift of the absorption and photoluminescence maxima of the NCs towards longer wavelengths. The shift is explained by partial tunnelling of electron wavefunction into the shell formed. The improvement of the photoluminescence parameters of the passivated NCs was found to be dependent on the total volume of the passivating material and the order of addition of Cd- (Zn-) and S-containing reagents. The maximum enhancement of the PL intensity by a factor of four was achieved for ZnS-passivated NCs. A considerable Stokes shift of the near-bandgap emission band was observed and its possible origin is discussed.

Acknowledgments

V Dzhagan is grateful to the Alexander von Humboldt Foundation for financial support during his research stay at Chemnitz University of Technology. The work was also partially supported by the Fundamental Researches State Fund of Ukraine.

References

[1] Peng X, Schlamp M C, Kadavanich A V and Alivisatos A P 1997 *J. Am. Chem. Soc.* **119** 7019
[2] Schmid G (ed) 2004 *Nanocrystals: From Theory to Application* (Weinheim: Wiley–VCH) and references therein
[3] Spanhel L, Haase M, Weller H and Henglein A 1987 *J. Am. Chem. Soc.* **109** 5649
[4] Wilson W L, Szajowski P J and Brus L E 1993 *Science* **262** 1242
[5] Kortan A R, Hull R, Opila R L, Bawendi M G, Steigerwald M L, Carroll P J and Brus L E 1990 *J. Am. Chem. Soc.* **112** 1327
[6] Hoener C F, Allan K A, Bard A J, Campion A, Fox M A, Mallouk T E, Webber S E and White J M 1992 *J. Phys. Chem.* **96** 3812
[7] Mews A, Eychmuller A, Giersig M, Schooss D and Weller H J 1994 *Phys. Chem.* **98** 934
[8] Danek M, Jensen K F, Murray B C and Bawendi G M 1996 *Chem. Mater.* **8** 173
[9] Hines M A and Sionnest P G 1996 *J. Phys. Chem.* **100** 468
[10] Pradhan N, Katz B and Efrima S 2003 *J. Phys. Chem.* B **107** 13843
[11] Raevskaya A E, Stroyuk A L, Kuchmiy S Ya, Azhnyuk Yu M, Dzhagan V M and Valakh M Ya 2006 *Theor. Exp. Chem.* **42** 150
[12] Raevskaya A E, Stroyuk A L, Kuchmiy S Ya, Azhniuk Yu M, Dzhagan V M, Yukhymchuk V O and Valakh M Ya 2006 *Colloids Surf.* A **290** 304
[13] Brus L 1986 *J. Phys. Chem.* **90** 2555
[14] Yu W W, Qu L, Guo W and Peng X 2003 *Chem. Mater.* **15** 2854
[15] Rogach A L, Kornowski A, Gao M, Eychmüller A and Weller H J 1999 *Phys. Chem.* B **103** 3065
[16] Schooss D, Mews A, Eychmüller A and Weller H 1994 *Phys. Rev.* B **49** 17072
[17] Chestnoy N, Harris T D, Hull R and Brus L E 1986 *J. Phys. Chem.* **90** 3393
[18] Pesika N S, Stebe K J and Searson P C 2003 *J. Phys. Chem.* B **107** 10412
[19] Kuno M, Lee J K, Dabbousi B O, Mikulec F V and Bawendi M G 2003 *J. Chem. Phys.* B **106** 9869
[20] Ma X-D, Qian X-F, Yin J, Xi H-A and Zhu1 Z-K 2002 *J. Colloid Interface Sci.* **252** 77

[21] Ivanda M, Bischof T, Lemann G, Materny A and Kiefer W 1997 *J. Appl. Phys.* **82** 3116
[22] Dabbousi B O, Rodriguez-Viejo J, Mikulec F V, Heine J R, Mattoussi H, Ober R, Jensen K F and Bawendi M G 1997 *J. Phys. Chem.* B **101** 9463
[23] Baranov A V, Rakovich Yu P, Donegan J F, Perova T S, Moore R A, Talapin D V, Rogach A L, Masumoto Y and Nabiev I 2003 *Phys. Rev.* B **68** 165306
[24] Dzhagan V M, Valakh M Ya, Raevskaya A E, Stroyuk A L, Kuchmiy S Ya and Zahn D R T 2007 *Nanotechnology* at press
[25] Xu L, Wang L, Huang X, Zhu J, Chen H and Chen K 2000 *Physica* E **8** 129
[26] Yu Z, Li J, O'Connor D B, Wang L-W and Barbara P F 2003 *J. Phys. Chem.* B **107** 5670
[27] Liu S-M, Guo H-Q, Zhang Z-H, Li R, Chen W and Wang Z-G 2000 *Physica* E **8** 174
[28] Efros Al L, Rosen M, Kuno M, Nirmal M, Norris D J and Bawendi M G 1996 *Phys. Rev.* B **54** 4843
[29] Norris D J, Efros Al L, Rosen M and Bawendi M G 1996 *Phys. Rev.* B **53** 16347
[30] Nirman M, Murray C B and Bawendi M G 1994 *Phys. Rev.* B **50** 2293
[31] Norris D J, Nirman M, Murray C B, Sacra A and Bawendi M G 1993 *Z. Phys.* D **26** 355
[32] Malý P, Kudrna J, Trojánek F, Mikeš D, Němec P, Maciel A C and Ryan J F 2000 *Appl. Phys. Lett.* **77** 2352
[33] Wang Q, Pan D, Jiang S, Ji X, An L and Jiang B 2006 *J. Lumin.* **118** 91
[34] Li J J, Wang Y A, Guo W, Keay J C, Mishima T D, Johnson M B and Peng X 2003 *J. Am. Chem. Soc.* **125** 12567
[35] Talapin D V, Rogach A L, Kornowski A, Haase M and Weller H 2001 *Nano Lett.* **1** 207
[36] Bawendi M G, Carroll P J, Wilson W L and Brus L E 1992 *J. Chem. Phys.* **96** 946
[37] Wang X, Qu L, Zhang J, Peng X and Xiao M 2003 *Nano Lett.* **3** 1103
[38] Lodahl P, van Driel A F, Nikolaev I S, Irman A, Overgaag K, Vanmaekelbergh D and Vos W L 2004 *Nature* **430** 654
[39] Woggon U, Herz E, Schops O, Artemyev M V, Arens Ch, Rousseau N, Schikora D, Lischka K, Litvinov D and Gerthsen D 2005 *Nano Lett.* **5** 483
[40] Petrov E P, Cichos F and von Borczyskowski C 2006 *J. Lumin.* **119/120** 412
[41] Dzhagan V M, Valakh M Ya, Raevskaya A E, Stroyuk A L, Kuchmiy S Ya and Zahn D R T 2007 *Appl. Surf. Sci.* at press